UDK621.3:(53+54+621+66), ISSN0352-9045 Informacije MIDEM 36(2006)1, Ljubljana

SILICON OPTICAL MICROSTRUCTURES BASED ON WET MICROMACHINING

D. Resnik, D. Vrtačnik, B. Batagelj*, U. Aljančič, M. Možek, S. Amon

University of Ljubljana, Faculty of Electrical Engineering, Laboratory of Microsensor Structures and Electronics, Ljubljana, Slovenia

*Radiation and Optics Laboratory, Ljubljana, Slovenia

Key words: silicon micromachining, surfactant, beam splitters, micro mirrors, roughness

Abstract: Optical microstructures were designed and fabricated with the purpose of out-of-plane and in-plane light beam manipulation. Microstructures were realized on {100} silicon with improved wet etching technique. Successful implementation of Triton-x-100 surfactant as an additive to the 25%TMAH-water etching system is reported, resulting in improved etching anisotropy and realization of smooth {110} silicon crystal planes, representing 45° mirrors. For in-plane reflections, thin {010} vertical walls were realized, serving as beam splitters or mirror reflectors. Fabricated microstructures were characterized in order to obtain information on the morphology of reflecting planes and their optical properties at three wavelengths.

Silicijeve optične mikrostrukture realizirane z mikroobdelavo

Kjučne besede: silicij, mikroobdelava, surfaktanti, mikrozrcala, delilniki, hrapavost

Izvleček: V prispevku so predstavljene optične mikrostrukture, realizirane na {100} siliciju s postopki anizotropnega mokrega jedkanja. Načrtane in izdelane so bile mikrostrukture, ki omogočajo manipulacijo svetlobnega žarka tako v {100} ravnini, kot tudi pravokotno navzven. Z dodatkom Triton-x-100 surfaktanta pri mokrem jedkanju silicija s 25%TMAH jedkalom smo dosegli izboljšanje anizotropije med posameznimi kristalnimi ravninami, kar nam je omogočilo realizacijo 45° zrcal z izredno gladkimi {110} površinami. Za manipulacijo žarka v ravnini so bila izdelana vertikalna zrcala, omejena z {010} kristalnimi ravninami, ki služijo kot odbojne površine ali polprepustni delilniki vpadnega žarka. Izvedena je bila optična in morfološka karakterizacija izdelanih mikrostruktur.

1. Introduction

Integration of MEMS and micro-optics has created a new class of microsystems, termed micro-opto-electro-mechanical systems (MOEMS), covering a very broad spectrum of microsystems and functionalities, from telecommunications and optical instrumentation to imaging systems. Excellent survey on the state of the art MOEMS was given recently by Motamedi /1/.

Optical communications require various types of light beam manipulations that can be realized monolithically on a single silicon optical bench. This approach enables integration of mechanical, electrical and optical components and functions in a single complex microstructure, resulting in improved performance and reduced cost. Furthermore, it is expected for the future that many electrical connections on/between chips will be replaced by optical waveguides.

In parallel optical communications, aligning of optical fibres to a second group of elements with low coupling losses is a demanding task. One segment of optical links where the losses can be optimized are reflecting mirrors, reflecting the in-plane to the out-of plane optical signal, or vice versa. Monolithic optical silicon benches with micromachined mirrors that meet demands for desired reflecting angle and low beam scattering, in conjunction with appropriate *U* or *V* shaped fibre aligning grooves are an attractive solution /2/. Compared to {111} crystal planes where mirror is under 54.74° with respect to the {100} surface, the {110} mirror planes with an angle of 45° toward surface allow more efficient coupling with single mode fibres having a small angle of acceptance /3,4/.

In our study, beside standard IPA additive to TMAH etchant, nonionic surfactant Triton-x-100 is investigated as an additive to the TMAH etching solution to improve the anisotropy ratio. Besides, Triton is also commonly used in the microelectronics processing. Another advantage over IPA is that the etching temperature can be increased due to higher boiling point of Triton. Our investigation was carried out by adding small amounts of Triton to the 25%TMAH-water etchant in the range of 0.1-1000ppm.

Monolithic optical benches were designed and fabricated to allow the characterization of etching parameters. Designed benches included 45° mirrors for out-of- plane reflection, corner splitters as well as vertical walls bounded by {010} planes for in-plane manipulation of light beam. Experimental validation of these planes was performed by measurement of angles and intensity profiles of reflected beams as well as by measuring the morphological parameters of reflecting planes.

By applying two step anisotropic etching (mask/maskless) we found a possibility of obtaining reflecting planes with

very low angle. In this case the mirror planes are {311}, with the angle of 25.24° toward {100} surface. By implementing our original approach, it is also shown that a mirror composed of {111} and {311} plane can be fabricated, thus acting as a beam splitter.

Optical mirror planes are characterized by several quality factors, most important being the degree of reflectance and dispersion angle of reflected light. Dispersion of reflected light is a function of mirror surface microroughness which causes scattering, the fibre distance from the mirror and the numerical aperture of single mode fibre. Optimal conditions for implementation of Triton, such as agitation, etch rates, anisotropy and surface roughness were investigated.

2. Experimental work

The experimental work was carried out on a low resistivity (1-5Ohmcm), n-type, single side mechanically polished float zone (FZ) silicon wafers with <001> crystal orientation (Topsil). Silicon wafers were thermally oxidized at 975°C to grow 600nm of SiO_2 and some were additionally covered with 70nm of LPCVD nitride (Si_3N_4) deposited at 800°C, to provide accurate masking against aggressive etchants.

Chromium mask was designed to fabricate optical bench microstructures (10x10mm^2) with parallel fibre grooves of different widths (240-400μm) and 200μm pitch between them (see Fig.5). Designed *V* grooves were terminated with mirror at one side of the groove and with open end on the opposite side to insert the fibre. Mask orientation versus primary wafer flat determines the sidewall angle of the groove and the slope of end mirror toward the surface plane and was chosen according to the requirements of the microstructure functionality.

Wet anisotropic micromachining of photolithogaphically defined areas was performed in 25%TMAH -water solution (Honeywell) and also in 33%KOH-water solutions in some cases.

A new additive, which was used with TMAH in our experiments, the non-ionic surfactant (i.e. surface active agent) Triton-x-100, is a mild surfactant often used in biochemical applications. Chemically, this additive is a stable octylphenol-ethyleneoxide condensate (Union Carbide). Beside compatibility with CMOS processes, the advantage of Triton-x-100 is higher boiling temperature point compared to IPA. This enables etching at higher temperatures, thus reducing the etch time.

Samples were etched in a closed thermostated (±1°C) glass vessel with the total content of 500ml of etching solution, with agitation by a magnetic stirrer in the temperature range 70-100°C.

Geometrical dimensions and accordingly the etch rates were determined by measuring lateral distances under the microscope. Surface quality, described by average roughness *Ra*, was evaluated by Taylor-Hobson surface profiler and surface morphology was characterized by AFM, SEM and optical microscope.

Fabricated benches and mirrors were characterized optically by measuring the beam dispersion angle and by analyzing the intensity profile of reflected beam. Fibres used in characterization setup were standard single mode fibres with diameter 125μm and numerical aperture NA=0.12. The intensity of reflected beam was measured at three wavelengths: 632nm (HeNe laser), 1.33μm and 1.54μm (Fabry-Perot type laser diodes).

3. Results and discussion

3.1. The role of additives in the etching process

In a manner to reveal {110} crystal planes on commonly used (100) silicon wafers, two conditions have to be met simultaneously. The first is that the structures are oriented at 45° toward the <110> oriented wafer flat and secondly, additives to the anisotropic etchant are essential to properly adjust the anisotropy ratio.

It is known that IPA additive to KOH or TMAH /5,6/ does not affect significantly the {100} etch rate; however, it does decrease {111} and {110} etch rates and therefore also anisotropy. It was shown recently that not only IPA, but also other alcoholic moderators have similar effect /7/.

Another type of additives was reported by Sekimura /8/ showing that small amounts (0.2%) of added surfactant NCW-601 to 22% TMAH solution exhibits improved surface performances for fabricated {110} planes with roughness Ra=100nm. Anisotropy and convex corner underetching were improved in both cases as well as surface roughness of {100} and of {110} planes. Presented work is focused on detailed investigation of TMAH-Triton etching parameters in order to obtain smooth {110} crystal planes with good anisotropy.

3.2. Effect of Triton-x-100 additive

Surfactants generally tend to accumulate and/or adsorb at solid-liquid interface, thus decreasing the contact angle between solid (silicon) and aqueous phase (anisotropic etchant). Triton surfactant acts as modifier of etchant surface tension. It is also very likely that Triton enters also in the polymerization process of the etching products by surrounding the etching products with the hydrated layer. This layer acts as a steric barrier to particle coalescence /9/. It is presumed that these effects play also a role in the observed etching characteristics. Etching experiments were performed with Triton content in the range 1-1000 ppm added into the 25% TMAH-water solution and optical bench samples were finally etched in the temperature range from 70-100°C.

In our previous work /10/, significant increase of etching anisotropy ratio $R_{(100)}/R_{(110)}$ was found in the range 10-

200ppm of added Triton to 25%TMAH. Over three orders of magnitude of added Triton (1-1000 ppm) very small variations of {100} crystal plane etch rate $R_{\{100\}}$ were observed. Major contribution to the increased anisotropy is a reduction of lateral etch rate $R_{<100>}$ which is related to $R_{\{110\}}$ ($R_{\{110\}}=R_{<100>}/\sqrt{2}$).

Minor influence of Triton on the $R_{\{100\}}$ etching rate is comparable to IPA influence observed by Merlos /5/ in the case of TMAH-IPA (reduction of 10 %). Compared to pure 25 % TMAH-water system, it was found that the {100} etch rate difference at these three temperatures is less than 15%. It was determined that the anisotropy ratio also increases with the increased etch temperature, mainly due to smaller increase of $R_{\{110\}}$ compared to $R_{<100>}$. Anisotropy ratio of 3.6 is achievable, which is much higher than for TMAH-IPA or KOH-IPA (0.9 and 1.8, respectively).

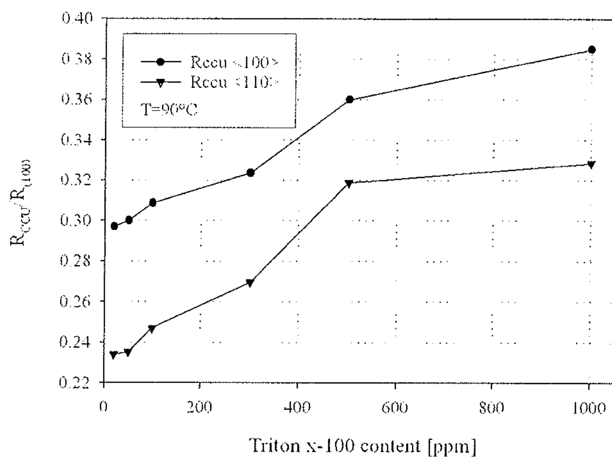

Fig.1. Normalized convex corner underetching for corners oriented in <110> and <100> direction for TMAH-Triton (50ppm) etching system.

Important figure of merit for an etching system in micromachining of silicon microstructures is low convex corner underetching. This phenomenon is more severe for structures having convex corners pointing in <100> direction compared to corners pointing in <110> direction. In our optical microstructures both directions are implemented and were investigated for TMAH-triton etchant. The corner underetching rate R_{CCU} was measured for both types of corners and then normalized by $R_{\{100\}}$ etch rate as shown in Fig.1. This ratio indicates how efficient is a specific etching system in preserving convex corners within the original shape during the etching process. Dependence of $R_{CCU}/R_{\{100\}}$ ratio on Triton content as presented in Fig.1 demonstrates that low content of Triton is favorable for decreasing the underetching in both cases. For the microstructures oriented in <100> direction having convex corners oriented in <110>, only etched bottom of corner is rounded while on the mask level, convex corner is completely preserved.

3.3. Influence of agitation on roughness (Ra) and etch rate R

To study the nature of etching mechanism in the presence of Triton and to distinguish whether the reaction is diffusion limited or surface reaction limited, the investigation was performed, how the agitation of the solution in the range from moderate (10rpm) to vigorous (900rpm) affects the etch rate of silicon. Therefore, etching in TMAH-triton (50ppm) at 90°C and equal etch time was chosen for all samples (60min). Results are shown in Fig.2. By measuring the {100} etch rates it was determined that the solution agitation does not influence severly the latter, and that the etching process is therefore almost surface reaction limited. However, lateral etch and therefore {110} plane etch rate $R_{\{110\}}$ show strong dependency on the agitation and points toward the diffusion controlled etching process in the presence of Triton. As well, convex corner underetching as a function of agitation was monitored for both directions, (<110> and <100>, respectively). Convex corners pointing in <110> direction were not influenced by agitation. However, corners pointing in <100> direction were significantly affected by agitation, i. e. corner high index crystal planes show diffusion limited behaviour.

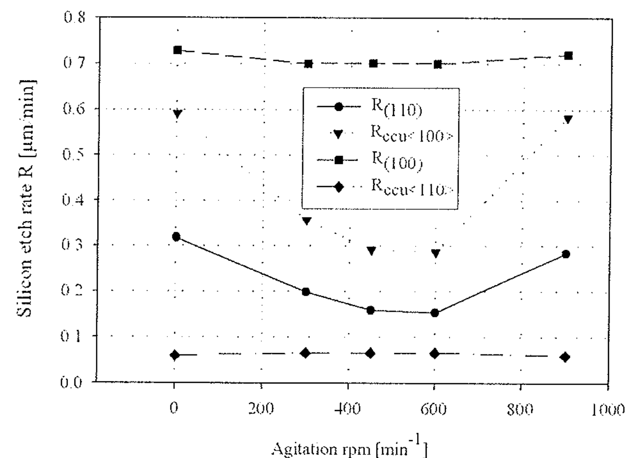

Fig.2. Dependency of vertical and lateral silicon etch rates on the agitation of TMAH-Triton (50ppm) solution at 90°C.

Regarding the surface quality of the reflecting {110} crystal planes etched by 25%TMAH-50ppm Triton-x-100, the agitation of the solution showed significant influence on *Ra*. Average roughness *Ra* is given by arithmetical mean value and was measured by surface profiler. At least four measurements on each sample were performed and etch experiments were repeated three times with fresh solutions. Therefore, results presented are an average of 12 measurements. It must be stressed that cut-off lenght (scan length) must be the same to obtain consistent results. Fig.3. shows that for the etching setup used, the most suitable range, where almost three times better {110} surface smoothness can be obtained is around 600rpm. Surface roughness appears as paralell elongated pits. Interplay beween the

mechanism of fresh solution reaching the interface and disturbance of turbulent flow at the interface result in homogeneous etching with low *Ra*.

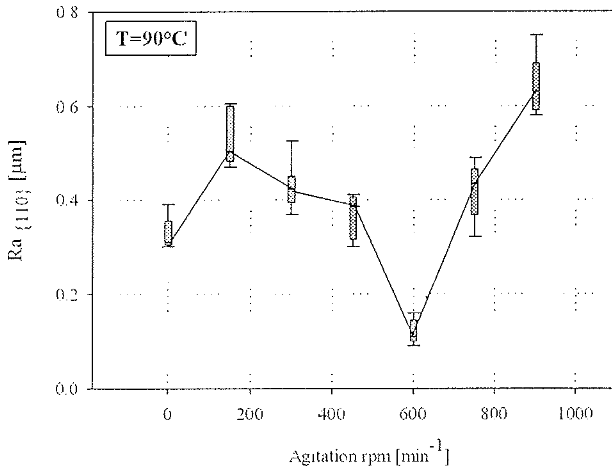

Fig.3. {110}crystal plane roughness vs. agitation of TMAH-Triton (50ppm) solution.

3.4. Activation energy of {110} and {100} plane

Beside TMAH-Triton, two other etching systems were taken into consideration, which also enable the formation of {110} planes. Activation energy for TMAH-Triton was established experimentally by measuring temperature dependence of etch rate for two planes of interest, i.e. {100} and {110}. The removal of silicon atoms is mainly a consequence of sufficient activation energy of the etching species. Arrhenius plot presented in Fig.4 shows the measured temperature dependency of etch rate for both crystal planes. From these plots activation energies for different etchants were derived, taking into account the well known Arrhenius expression ($R=k.exp(-Ea/RT)$). Here, R is the measured etch rate of specific crystal plane, *k* is the pre-exponential factor corresponding to the total number of the events and *Ea* is the activation energy. *Ea* is actually proportional to the number of molecules which are capable of removing Si atoms from the surface. This, so called, collision theory is, however, not sufficient to explain the activation energy differences when using different additives. By introducing activating complex theory, which is describing the transition state of the reaction, Ea corresponds to the molar enthalpy of the reaction and the factor *k* represents the molar entropy of the activation process /11/. Due to the fact that the reaction and transport take place in a solution, which affects events macroscopically, the explanation is even more complicated. Beside sufficient energy of reactant species,

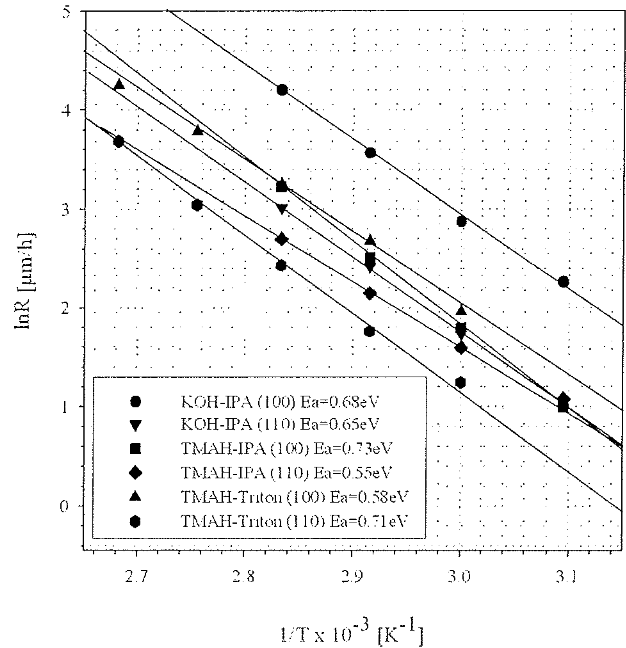

Fig.4. Arrhenius plot showing temperature dependency of etch rates of {110} and {100} planes, for three etchants.

the orientation of species necessary for the reaction and the necessary distance is important as well.

Calculated highest activation energy for TMAH-Triton-50ppm (0.71eV) is in a good correlation with significant increase in anisotropy which is actually a consequence of reduced {110} etch rate. The lowest activation energy for {110} plane exhibits TMAH-IPA etching system, what complies with highest {110} etch rate. KOH-IPA activation energy is in-between, but with very rough surface (Ra>200nm). At lower temperatures it was observed that etch rates were inhibited, probably due to prevailed growth of passivation oxide layer. Table1 presents values of activation energies and preexponential factors, derived from measurements of etch rates for two crystal planes and three etching solutions of interest.

Triton is affecting the accessibility of etching species toward preferential crystal planes which have more open network structure, such as {110} and higher index planes. Probably it plays a role also in the removal of etching products at the interface of {110} plane more dominantly compared to {100} interface Additional factors, such as polarity effects of surfactant, which are connected to binding energy on the specific preferential planes, angle and type of bonds may also affect the characteristics of Triton-etchant-silicon system /12/.

Table 1: Calculated activation energies and pre-exponential factors

	KOH-IPA {100}	KOH-IPA {110}	TMAH-IPA {100}	TMAH-IPA {110}	TMAH-TRITON {100}	TMAH-TRITON {110}
Ea [eV]	.683	.651	.735	.553	.579	.709
Preexp.factor	3.74E11	3.94E10	7.56E11	1.14E9	4.64E9	1.47E11

3.5. Fabrication of optical benches

Three different types of optical benches were designed and fabricated on (100) silicon substrate. First optical bench was designed for aligning out-of-plane mirrors and optical fibres, where fibres enter the optical bench from the same direction (Fig.5a). Second optical bench was designed for optical fibres entering from both directions, where V grooves and the out-of-plane 45° mirrors are interdigitated (Fig.5b). In the third optical bench design, four optical functions were taken into considerations with in-plane light paths (Fig.5c). This optical bench enables function of corner beam splitter and function of retroreflection (reflecting light beam of 180°) in {100} plane. Furthermore, the structure of thin vertical {010} wall beam splitter should enable partial reflection and partial transmission of the input light signal, depending on the wavelength and angle of incidence. However, due to limitations in the etching process (anisotropy, roughness) it is not always possible to provide simultanousely good performances for all of the above functions in the same etching system.

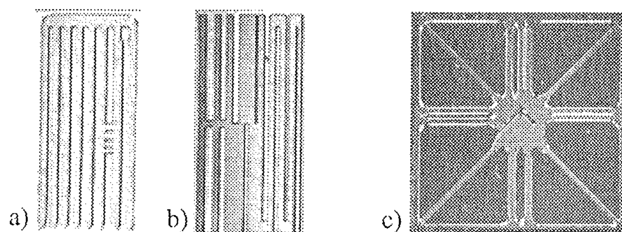

Fig.5. Three different designed and fabricated monolithic silicon optical benches with fibre grooves and reflecting mirrors (a,b-size $5x10mm^2$, c-size $10x10mm^2$).

3.5.1. {110} crystal plane mirrors

On the basis of etching experiments and measurements, optimal conditions were chosen for a fabrication of 45° mirrors. TMAH-Triton (50ppm) at temperature 90°C and agitation of 550rpm was selected. Fig.6a presents a detail of the fabricated groove terminating with a broad {110} mirror. Grooves are 130µm deep, sufficient to accommodate single mode fibres. The micromachined peninsulas formed by superposition of squares (convex corners in <110> direction) at each side of the groove are dedicated to limit the lateral movement of inserted fibre and can be well trimmed with etching process parameters

Additionally, in Fig.6b fibre and beam reflection is also illustrated to obtain clear view of light path and beam widening for the standard groove and mirror. Fig. 6c is presenting 45° mirror with recorded beam pattern of reflected 632nm light. Beam width angle b is estimated to 25°. Fibre with NA=.12 corresponds to beam width of 15.3°, thus the difference 10° is due to scattering. Surface roughness for TMAH-Triton system of these mirrors was measured by AFM. Average roughness *Ra* was between 6-14nm and the appearance of shallow, elongated pits is significantly minimized.

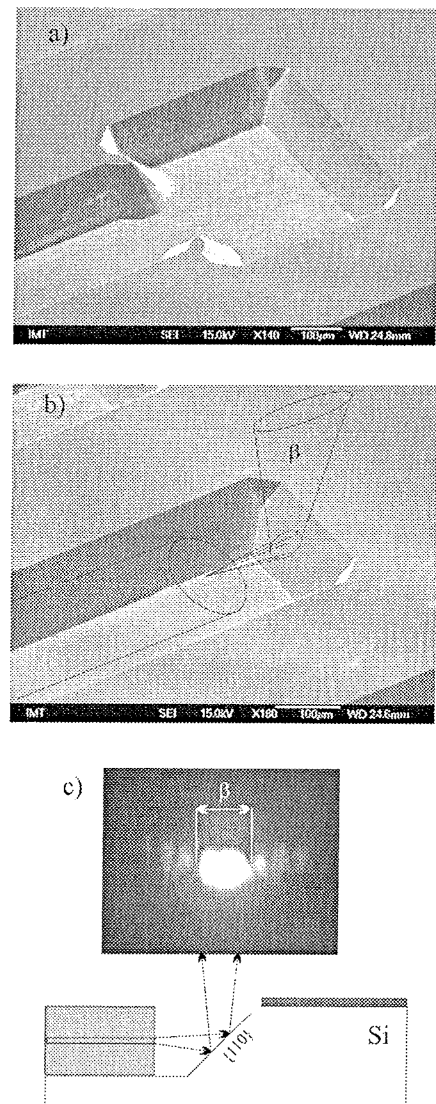

Fig.6. Detail of the groove, ending with {110} mirror plane (a) and design accompanied with a structure for precise horizontal aligning (b), etched by TMAH-Triton-x-100 (50ppm), while (c) shows pattern of the reflected out of plane beam.

In the mirror applications, reflectance is a dominant parameter. If mirror is perfectly flat, then only specular reflectivity, which is a function of material properties (refractive index *n* and extinction coefficient *k*), is expected. Specular reflectivity of bare Si is around 35% at 628nm (31%, 32% at 1.33 and 1.54µm, respectively). According to measurements made by Uenishi, reflectance increases with increasing angle of incident light; at incident angle of 45°, the reflectivity is around 0.5 /13/ and according to Zou /14/ around 0.4 at 632nm for bare silicon substrate. By covering the reflecting planes with highly reflective metals such as gold or aluminum, the reflectivity of mirror can be increased /14,15/. In our experiments, 50nm thick sputtered Au layer on the silicon mirror surface was used as reflective surface on 45° mirrors. This thickness exceeds greatly the required minimal skin depth. Au exhibits an overall specular reflec-

tivity of 97.5% at 632nm and above for higher incident wavelengths /15/.

In reality, the reflective surface is rough by nature and this results in additional reflective component losses due to diffused reflection (light scattering). Light scattering is mainly determined by surface microroughness, incident angle and wavelength of incident light. To estimate the reduction of reflectivity due to scattering component, ratio of scattering component vs. total reflected light can be calculated by the following expression (1) from the scalar scattering theory /16/:

$$\frac{P_{scat}}{P_{tot}} = 1 - e^{-\left(\frac{4\pi Ra\cos\theta}{\lambda}\right)^2} .100 \text{ [\%]} \qquad (1)$$

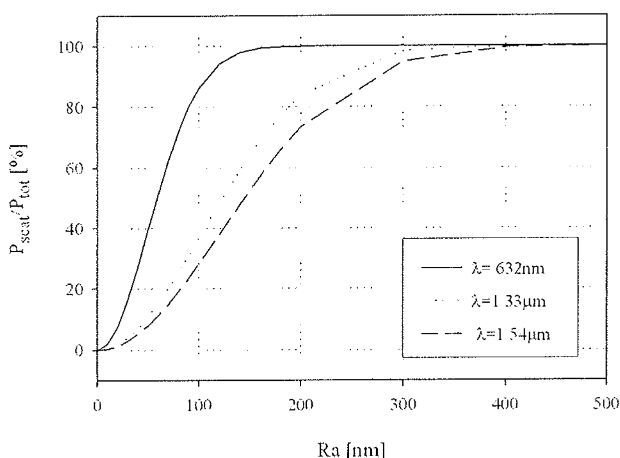

Fig.7. Influence of mirror surface roughness Ra *on the scattering component of reflected light.*

According to Cochran /15/, *Ra* values that are three orders of magnitude less than operating wavelength are acceptable. Tradeoffs are needed between the mirror surface quality and compatible processes required to finalize the whole microstructure. Fig.7 shows the scattering light contribution with respect to increased mirror roughness *Ra* for three wavelengths taken into account in our study. Roughness is more severely involved in scattering toward lower wavelengths. For measured values of our samples, realized with optimal Triton conditions (*Ra* between 5-14nm), the expected scattering part should be below 5 % for the 632nm and even less for higher two wavelengths. The overall measured out-of-plane intensity for Au coated mirrors was about 73% of incident light at 632nm and 78 to 80% for 1.33μm and 1.55μm, respectively. Additional losses are attributed to air-fibre interface (6.8% according to Cochran /15/) and geometrical misalignment. According to measured intensities, roughness of some samples was probably higher than shown by AFM results on small scale.

3.5.2. {111}/{311} crystal plane splitter

When the microstructures are oriented in <110> direction, mirrors with angle 54.74° toward surface are obtained. Using two step etching (mask/maskless) with 25%TMAH etchant, also grooves and mirrors with {{311}} sidewalls and corresponding angle of 25.24° toward surface are viable /17/. Interesting features can be obtained by combining the {111} and {311} planes as a reflective slopes on (100) silicon bench.

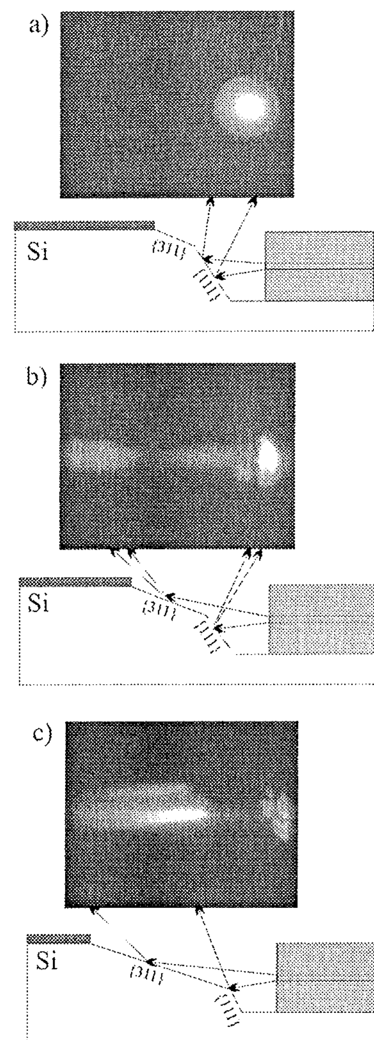

Fig.8. Beam patterns obtained from three different stages of micromachining combined {111}/{311} crystal plane splitter.

By implementing this approach, the incident beam can reflect from two slopes and two out-of-plane beams can be obtained. Fig.8 is presenting this principle together with images of reflected optical beam which is detected on transparent screen, located parallel and above the optical bench. Fig.8a corresponds to the situation where {311} is just formed and most of the slope is still {111} plane giving symmetrical Gaussian beam pattern. After further etching, {311} plane prevails by consuming the {111} plane. This is seen as reduced image from {111} and elongated image appears from {311} (Fig.8c). By accurate fabrication of the two planes in a desired height ratio, one can tailor the splitter by the actual requirements. AFM results for {311} and {111} planes are shown in Fig.9 and can be validated by means of *Ra* values.

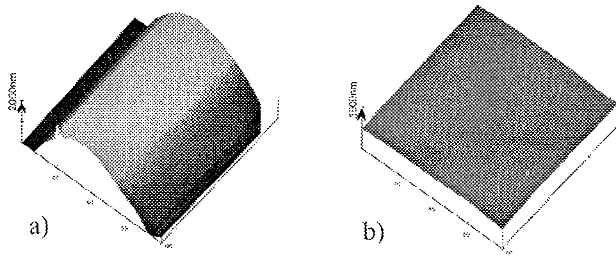

Fig 9. AFM 3D image of 80x80 μm^2 mirror area of combined {111}/{311} crystal plane splitter (a) {311} plane with Ra=*180nm and (b) {111} plane with* Ra=*2.9nm*

As reported earlier /17/, and shown as well on the AFM 3D plot (Fig.9), slightly convex shape is obtained, which causes the dispersion of reflected beam shown above. Consequently the optical losses are quite high. However, the distortion of reflected pattern from {311} is difficult to annulate. Beam width is proportional to the distance of fibre from the mirror and the numerical aperture of fibre. By correlating the screen pattern with AFM results, it is evident that the high scattering angle is the consequence of a pronounced convex contour rather than a local microroughness.

3.5.3. {010} wall beam splitter

To enable beam reflection in (100) plane, vertical mirrors are required. For such vertical {010} walls, design rules have to take into consideration all the predictive details determined earlier. To accomplish this kind of wall, KOH or TMAH anisotropic etchant have to be employed and mask must be oriented in <100> direction. To obtain partial reflection and partial transmission at particular wavelength, proper thickness has to be determined according to the material properties as will be shown in detail later in this section. Fig.10 shows SEM micrograph of fabricated central region of bench, showing vertical {010} wall, 15µm thick and 150µm high. SEM analysis have shown that wall fabricated by KOH reveals (010) plane with residuals on top and bottom level, while TMAH gives perfectly smooth {010} plane (see inset in Fig.10).

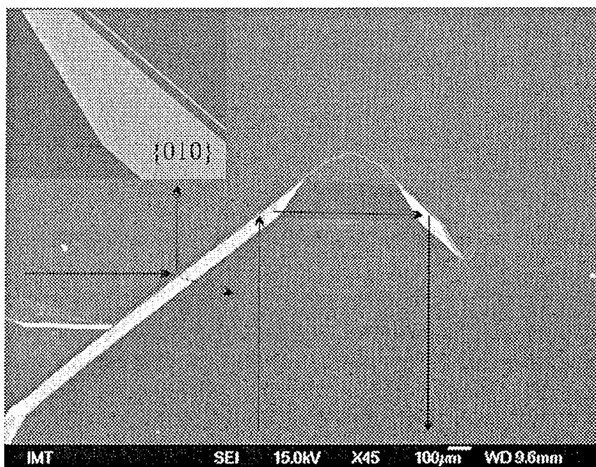

Fig.10. SEM micrograph of smooth vertical {010} wall (15µm thick, 130µm high), fabricated by 25%TMAH.

Fig.11 shows 90° reflection from silicon {010} vertical wall, with partial tranmission, depending on wall thickness and incident wavelength. Precise alignment of fibres is mainly a function of the design and is of utmost importance for minimizing optical losses.

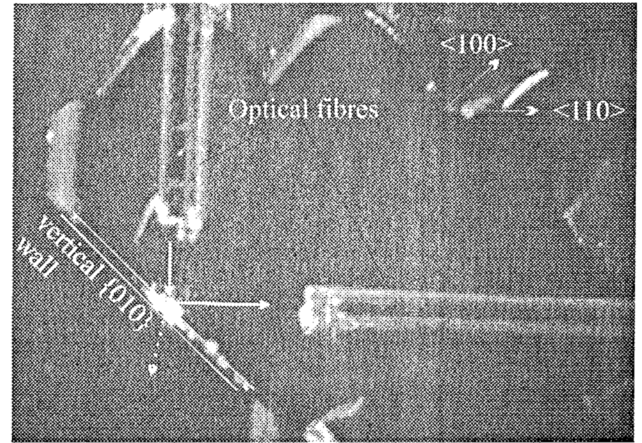

Fig.11. Detail of optical bench with designed in-plane beam 90° reflection from (010) wall

For the wavelengths in the range of 1.1-2.5µm, the absorption in silicon is very low. Therefore increased transmittance is governed by the following equation given by /18/ for the normal angle of incidence.

$$T = \frac{(1-R^2)e^{-\left(\frac{4\pi kx}{\lambda}\right)}}{1-R^2 e^{-\left(\frac{8\pi kx}{\lambda}\right)}} \quad (2)$$

where R is the reflectivity of Si, k is the extinction coefficient of Si, l is the wavelength of incident light and x is the thickness of Si {010} wall. According to the calculated dependency of transmittance vs. silicon thickness, as shown in Fig.12, vertical wall can act as an attenuator. Small amount of attenuation is expected for higher two wavelengts and

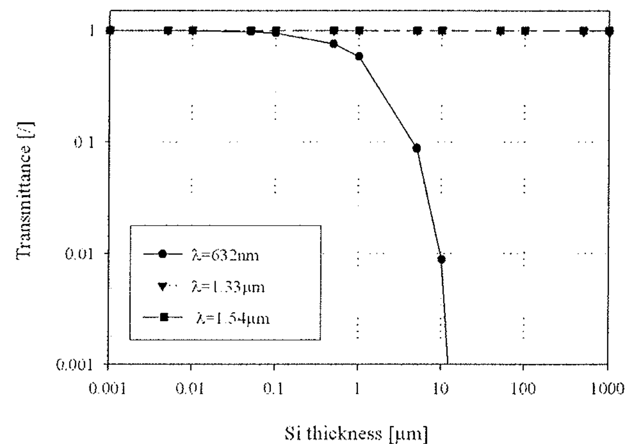

Fig.12. Calculated dependency of transmittance vs. silicon thickness, for three wavelengths (according to eq.2).

higher for 632nm (here, transmittance is reduced due to increased reflectivity and absorption). Attenuating configuration on the fabricated optical bench is presented in Fig.13. In this case, 15μm thick silicon transmits less than 0.1% of incident light intensity, what correlates well with the results of Uenishi /13/.

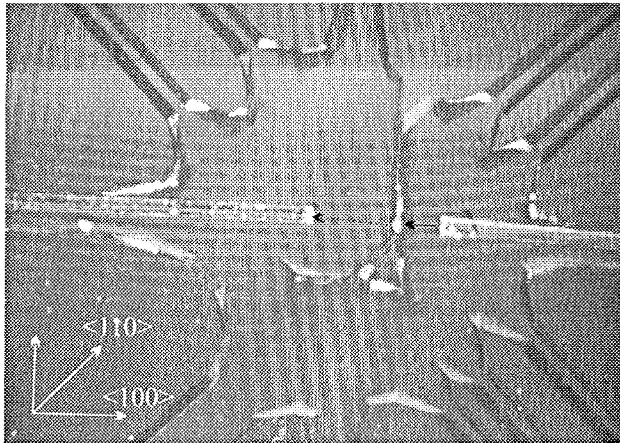

Fig.13. Detail of optical bench with designed in-plane attenuation through (010) wall.

3.5.4. Corner beam splitter

Optical microstructure, enabling in-plane division of incident beam, is also corner splitter, presented in Fig.14. To elaborate vertical {010} walls, meeting at right angle thus forming sharp convex corner, structure must be oriented in <100> direction. To avoid underetching, we designed square shaped compensation structure that resulted in relatively sharp convex corners. Two different etching solutions were investigated to obtain a sharp convex corner, which would provide perfect beam splitting without out-of-plane beam losses. By applying the TMAH etchant in the fabrication, the splitter convex corner was greatly improved compared to KOH. The optical paths for splitter microstructure were designed for 50μm wide and 130μm high {010} vertical wall. In this case the insertion loses between input and output fibres should be minimized. To obtain the ideal splitter 50:50, convex corner of two orthogonal {010} planes should have perfect edge and the fibres must be carefully aligned in the proximity of corner, which is in practice a very demanding task. Results of our measurements on this particular corner beam splitter as shown in Fig.14, showed that each of output fibres received only 20-25% of incident intensity at 632nm. According to Rosengren /19/, this corresponds to 3-4dB of optical losses. To minimize losses, improved compensation structure has to be designed, which will improve the corner quality even further. For quantitative evaluations, additional efforts are required also in terms of reduced misalignment of fibres.

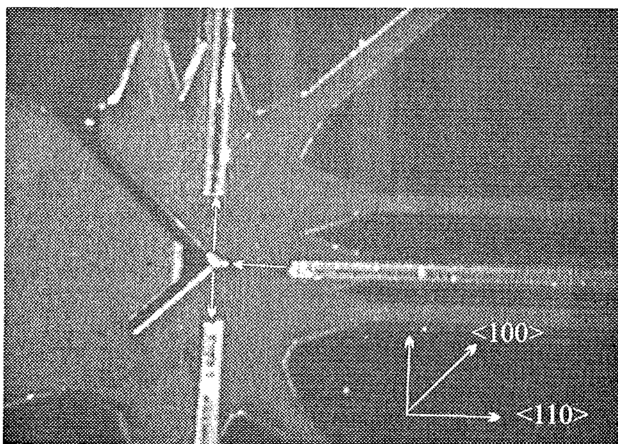

Fig.14. Detail of optical bench with corner beam splitter and inserted fibres.

3.6. Optical characterization of reflecting {110} mirrors

The setup for optical characterization of 45° mirrors at three wavelenghts consisted of light sources, collimator, *xyz* adjusting micromanipulators to achieve maximal coupling between the source and the optical fibre guide, detector and a microscope with CCD camera to enable precise fibre insertion in the grooves of optical bench (Fig.15).

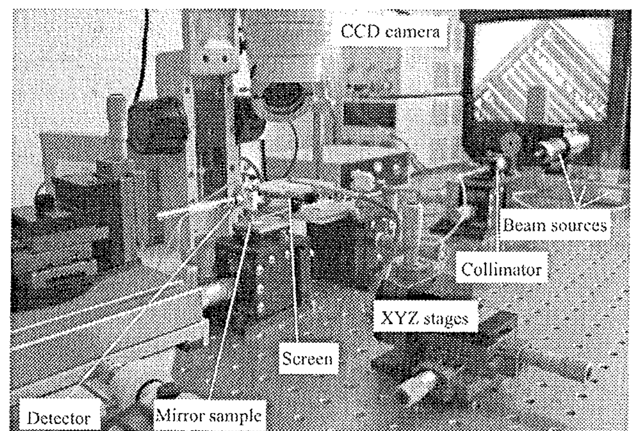

Fig.15. Optical characterization setup.

For 45° silicon mirrors, optical measurements with visible 632nm wavelength beam were first accomplished. Reflected light beam pattern, displayed on semitransparent screen positioned perpendicularly to the output beam at a fixed distance from the optical mirror, provided information about scattering angle, angle of out-of-plane deflection and also morphology of reflecting mirror, as shown in Fig.6c and Fig.8.

Mirrors were further characterized by scanning the *xy* plane perpendicular to the direction of the reflected beam by Si calibrated reference photodiode. Intensity of illuminated photodiode detector was measured with HP 3457A multimeter. In case of 1.33μm and 1.54μm wavelengths, Fabry-Perot type laser diode light sources were used and reflected beam intensity was determined by measuring the response of InGaAs photodetector.

Fig. 16 presents measured intensity profiles of reflected beam from {110} mirror (made by TMAH-Triton (50 ppm)) for three incident wavelengths. At 632nm, mirror has a very wide spatial response with FWHM value of angle nearly 35° and thus lower peak. The proportions of FWHM values are in a reasonable agreement with the results presented in Fig.6c where beam pattern was recorded on the semitransparent screen.

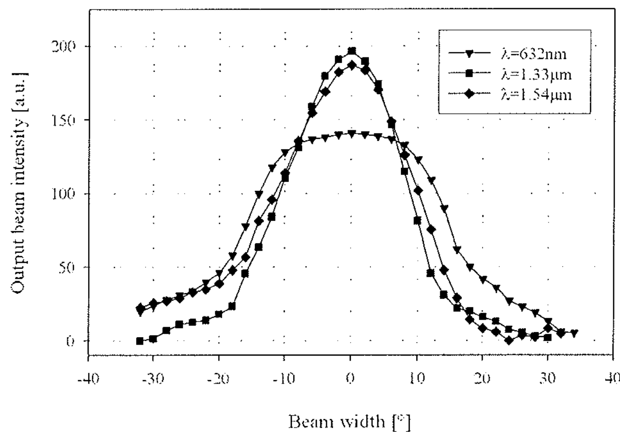

Fig.16. Intensity profiles of reflected output beams from {110} crystal planes. Mirrors were covered by 50nm of Au layer.

In case of incident beam wavelengths of 1.33μm and 1.54μm, what is substantially higher than the average roughness of reflecting crystal plane, it was expected, according to Fig.7, that microroughness does not play such a severe role as at lower wavelengths (*Ra*<<λ). By analyzing the profiles it can be seen that FWHM were decreased to values around 19° for both cases. Profiles are not fully symmetrical due to geometrical errors of fibre misalignment or *xy* scanning setup.

By correlating the results at 1.54μm and 1.33μm to those at 632nm wavelength, minor differences were revealed concerning reflected beam scattering angle at the two higher wavelengths. On the other hand, significant scattering was determined at the lowest wavelength, higher than expected from Fig.7. It is believed that this is due to poor end-face finish of the fibre (increased return losses) and due to additional modes present at 632nm wavelength.

Further work is needed to decrease optical losses, particularly those originating from mechanical misalignment (longitudinal, axial and angular) and from return losses due to poor fibre cut.

4 Conclusions

In the proposed study, optical microstructures realized on (100) silicon substrates with wet anisotropic etching were investigated. The implementation of Triton-x-100 surfactant in the range of 1-1000ppm to the 25% TMAH etchant is found to increase the anisotropy by decreasing the {110} etch rate and retaining the {100} etch rate. It was shown that surface roughness of {110} planes used as 45° optical mirrors is also greatly improved (*Ra*=6-14nm). In addition, convex corner underetching is strongly reduced. It was shown that TMAH-Triton system enables the formation of {110} mirror and fibre groove simultaneously. Optimal conditions for added content of Triton (50ppm) and stirring conditions (550rpm) were established to achieve smooth {110} mirrors. Activation energies of 0.58eV and 0.71eV for {100} and {110} planes, respectively, were determined.

Three types of optical microbenches were fabricated by wet micromachining, enabling out-of-plane and in-plane manipulation of light beam. Besides, important parameters such as roughness of reflecting mirror surfaces, transmittance of thin silicon {010} walls and spatial intensity distribution of reflecting beam were determined. Optical characterization of microbenches with incident light at wavelengths of 632 nm, 1.33 μm and 1.54 μm confirmed the functionality of the designed and presented microstructures.

Acknowledgments: This work was supported by Ministry of Higher Education, Science and technology of Republic of Slovenia.

References

/1./ M.E. Motamedi, editor, MOEMS, Micro-Opto-Electro-mechanical Systems, *SPIE Press*, Bellingham, USA, 2005.

/2./ M. Hoffmann, E. Voges, Bulk silicon micromachining for MEMS in optical communication system, *J. Micromech. Microeng.* 12, 349-360, 2002.

/3./ D. Sadler, M.J. Garter, C.H. Ahn, S. Koh, A.L. Cook, Optical reflectivity of micromachined {111} oriented silicon mirrors for optical input-output couplers, *J. Micromech. Microeng.* 7, 263-269, 1997.

/4./ C. Strandman, L. Rosengren, H.G.A. Elderstig, Y. Backlund, Fabrication of 45ş mirrors together with well defined V-grooves using wet anisotropic etching of silicon, *J. of Microelectromechanical Systems*, Vol. No. 4, December 213-219, 1995.

/5./ A. Merlos, M. Acero, M. H. Bao, J. Bausells, J. Esteve, TMAH-IPA anisotropic etching characteristics, *Sensors Actuators* A37-38, 737-743, 1993.

/6./ H. Seidel, L. Csepregi, A. Heuerberger and H.A. Baumgartel, Anisotropic etching of crystalline silicon in alkaline solutions, *J. Electrochem. Soc.* 11, 3612-3625, 1990.

/7./ W-J. Cho, W-K. Chin and C-T. Kuo, Effects of alcoholic moderators on anisotropic etching of silicon in aqueous potassium hydroxide solutions, *Sensors Actuators* **A** 116, 357-368, 2004.

/8./ M. Sekimura, Anisotropic etching of surfactant-added TMAH solution, *Proc. 21th IEEE Micro-Electro-Mech. Syst. Conf. (MEMS'99)* Orlando FL, Jan 17-21 650-55,1999.

/9./ A. Karagunduz, K.D. Pennel and M. Young, Influence of a nonionic surfactant on the water retention properties of unsaturated soils, *Soil Sci. Soc. of America J.* 65 1392-1399, 2001.

/10./ D. Resnik, D. Vrtacnik, U. Aljancic, M.Mozek, S. Amon, The role of Triton surfactant in anisotropic etching of {110} reflective planes on (100) silicon, *J. Microm. Microeng.*, 15, pp. 1174-1183, 2005.

/11./ P.W.Atkins, Physical Chemistry, Third edition, *Oxford University press*, 1986.

/12./ I. Zubel, The influence of atomic configuration of (*hkl*) planes on adsorption processes associated with anisotropic etching of silicon, *Sensors Actuators* A94, 76-86, 2001.

/13./ Y. Uenishi, T. Masahiro, M. Mehregany, Micro-opto-mechanical devices fabricated by anisotropic etching of (110) silicon, *J. Microm. Microeng.*, 5, pp. 306-312, 1995.

/14./ J. Zou, M. Balberg, C. Byrne, C.Liu, D.J. Brady, Optical properties of surface micromachined mirrors with etched hole, *J. Micromech. Microeng.* 8, 1999.

/15./ K.R. Cochran, L. Fan, D.L. DeVoe, Moving reflector type microoptical switch for high-power transfer in a MEMS- based safety and arming system, *J. Micromech. Microeng.* 14 2004.

/16./ M-Y. Jung, H. Ryu, M-L. Lee, C-H. Jun, Y.T. Kim, A novel process for high reflectivity of Al sidewalls of optical mirrors using KrF excimer laser annealing, *Proceed. of SPIE, Micromach. and microfabr. process technol. VII, 22-24.Oct S Francisco* 4557 111-118, 2001.

/17./ D. Resnik, D. Vrtacnik, S. Amon, Morphological study of {311} crystal planes anisotropically etched in (100) silicon: role of etchants and etching parameters, *J. Microm. Microeng.*, 10, pp. 430-439, 2000.

/18./ S.M. Sze, Physics of semiconductor devices, 2nd edition, *J.Wiley and sons*, N.Y. 1981

/19./ L. Rosengren, L. Smith, Y. Backlund, Micromachined optical planes and reflectors in silicon", *Sensors and Actuators*, A 41-42, 330-333, 1994.

doc.dr. Drago Resnik
doc.dr. Danilo Vrtačnik
*doc.dr. Boštjan Batagelj**
mag. Uroš Aljančič
mag. Matej Možek
prof.dr. Slavko Amon
University of Ljubljana, Faculty of Electrical Engineering,
Laboratory of Microsensor Structures and Electronics

**Radiation and Optics Laboratory*
Trzaska 25, Ljubljana 1000, SLOVENIA
E-mail: Drago.Resnik@fe.uni-lj.si

Prispelo (Arrived): 03. 01. 2006; Sprejeto (Accepted): 30. 01. 2006